AGU PUBLICATIONS

Geophysical Research Letters

RESEARCH LETTER
10.1002/2016GL071063

Key Points:
- First model of the structure of Knox Subglacial Sedimentary Basin of Wilkes Land
- Basin shown to result from India-Antarctic rifting in late Jurassic- Early Cretaceous
- Rift structure controls past erosion within Denman and Scott glacier catchment

Supporting Information:
- Supporting Information S1

Correspondence to:
A. R. A. Aitken,
alan.aitken@uwa.edu.au

Citation:
Maritati, A., A. R. A. Aitken, D. A. Young, J. L. Roberts, D. D. Blankenship, and M. J. Siegert (2016), The tectonic development and erosion of the Knox Subglacial Sedimentary Basin, East Antarctica, *Geophys. Res. Lett.*, *43*, 10,728–10,737, doi:10.1002/2016GL071063.

Received 23 JUN 2016
Accepted 14 OCT 2016
Accepted article online 15 OCT 2016
Published online 28 OCT 2016

The tectonic development and erosion of the Knox Subglacial Sedimentary Basin, East Antarctica

A. Maritati[1], A. R. A. Aitken[1], D. A. Young[2], J. L. Roberts[3,4], D. D. Blankenship[2], and M. J. Siegert[5]

[1]School of Earth and Environment, The University of Western Australia, Perth, Western Australia, Australia, [2]University of Texas Institute of Geophysics, The University of Texas at Austin, Austin, Texas, USA, [3]Australian Antarctic Division, Kingston, Tasmania, Australia, [4]Antarctic Climate and Ecosystems Cooperative Research Centre, The University of Tasmania, Hobart, Tasmania, Australia, [5]The Grantham Institute and Department of Earth Science and Engineering, Imperial College London, London, United Kingdom

Abstract Sedimentary basins beneath the East Antarctic Ice Sheet (EAIS) have immense potential to inform models of the tectonic evolution of East Antarctica and its ice-sheet. However, even basic characteristics such as thickness and extent are often unknown. Using airborne geophysical data, we resolve the tectonic architecture of the Knox Subglacial Sedimentary Basin in western Wilkes Land. In addition, we apply an erosion restoration model to reconstruct the original basin geometry for which we resolve geometry typical of a transtensional pull-apart basin. The tectonic architecture strongly indicates formation as a consequence of the rifting of India from East Gondwana from ca. 160-130 Ma, and we suggest a spatial link with the western Mentelle Basin offshore Western Australia. The erosion restoration model shows that erosion is confined within the rift margins, suggesting that rift structure has strongly influenced the evolution of the Denman and Scott ice streams.

1. Introduction

The study of the sedimentary basins of East Antarctica is of fundamental importance for understanding the tectonic processes that led to the breakup of East Gondwana and shaped the subglacial morphology of present–day Antarctica. [e.g. *Aitken et al.*, 2014, 2016a; *Close et al.*, 2007; *Espurt et al.*, 2012; *Frederick et al.*, 2016; *Gaina et al.*, 2007]. This is especially so for the Knox Coast, a region located at the Jurassic to Cretaceous triple junction of Greater India, Australia and East Antarctica [*Fitzsimons*, 2003]. Furthermore, the region hosts the Denman and Scott glaciers, which together drain a ~250,000 km^2 catchment within the East Antarctic Ice Sheet [*Rignot et al.*, 2011].

Unlike its conjugate Gondwana margins of Australia and Greater India, which have extensive datasets both onshore and offshore [e.g. *Bradshaw et al.*, 2003; *Chand et al.*, 2001], the onshore tectonic architecture of the Knox Coast region was virtually unknown until recently. New aerogeophysical data from the International Collaborative Exploration of the Cryosphere through Airborne Profiling (ICECAP) program traversed the continental interior, and allowed first interpretations to be made [*Aitken et al.*, 2014]. Those first interpretations identified a rift zone, the Knox Rift, with a deep sedimentary basin within it, the Knox Subglacial Sedimentary basin (KSSB). Spatial links with the Perth and/or Mentelle basins of the west Australian margin suggest that the Knox Rift may be a failed rift that developed during the rifting of India from East Gondwana.

The KSSB occurs within a ~150 km wide region, extending inland for over 700 km (Figure 1). This basin is characterized by low gravity anomalies (Figure 1a) and long-wavelength magnetic signatures (Figure 1b). Within the rift, deep and relatively smooth-based bed topography is interrupted by rugged highlands (Figure 1c). Depth to magnetic basement estimates indicate greater than 5 km sedimentary rock thicknesses beneath the ice sheet bed [*Aitken et al.*, 2014].

The regional subglacial landscape uncovered by the ICECAP data (Figure 1c) shows that most of the topography within the Knox Rift lies beneath sea level, reaching depths greater than 1 km in two regions located at 100 and 250 km inland from the present coastline. These basins are smooth-based at short wavelengths [*Wright et al.*, 2012]. The rift also contains significant topographic highs, over 1 km above sea level, and it is flanked to the east and west by high topography. These high-elevation regions possess rough bedrock topography [*Wright et al.*, 2012]. The topographic lows in the Knox Rift host the Denman

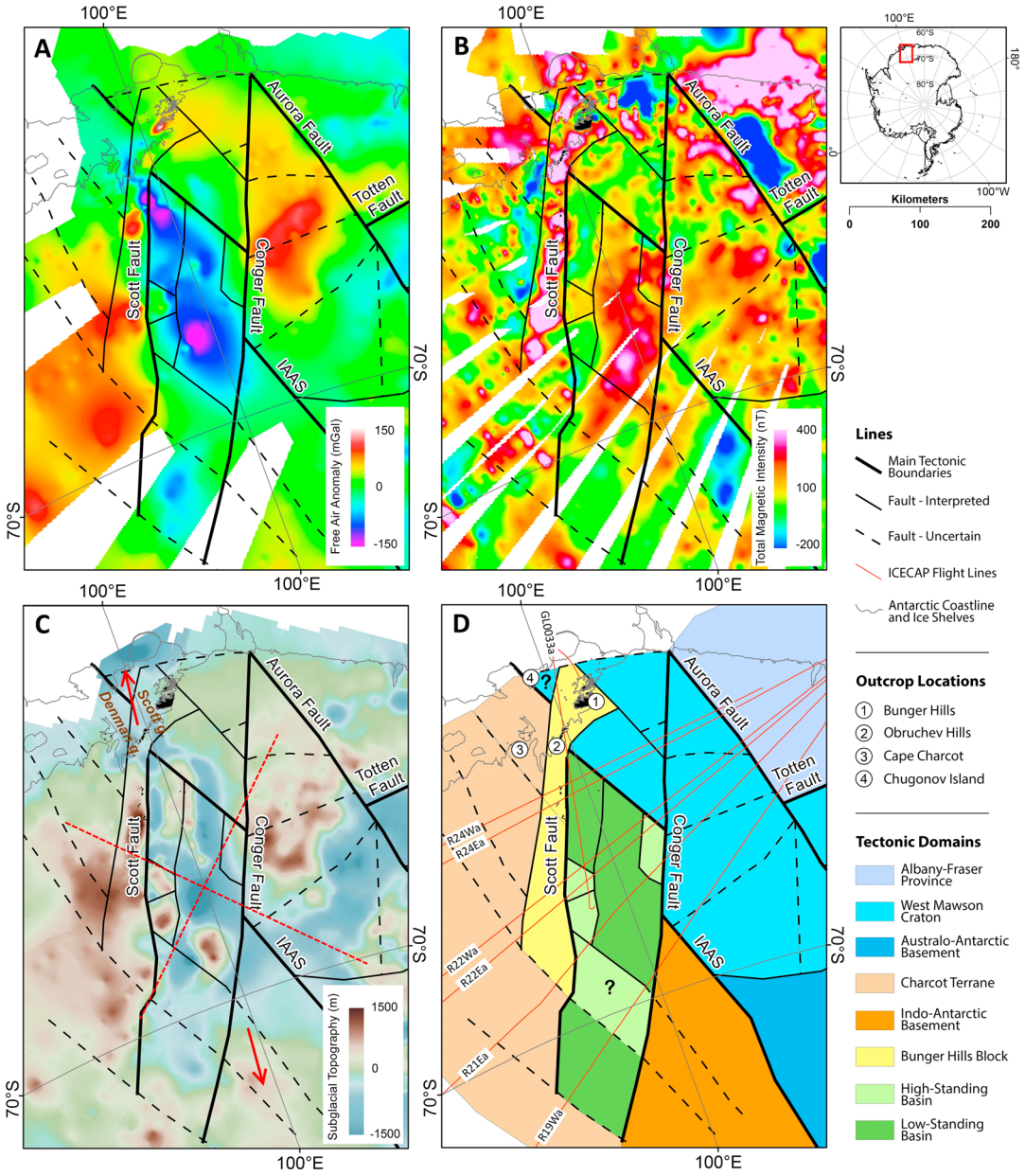

Figure 1. (a) Free-air gravity, (b) Total magnetic intensity, (c) Bedrock topography and (d) Our tectonic interpretation of the Knox Rift Region. Dashed red lines on (c) show "slip-lines" indicating the orientation and location of maximum shear-stress under conditions of N-S tension, and with a null-point in the center of the basin. Note how topography has high elevation in the compressional sectors and low elevation in the tensional sectors. Shearing and basin subsidence is focused along pre-existing structures oriented close to these slip-lines.

and Scott ice streams, which extend over 900 km into the continent interior, suggesting that rifting-induced differences in bed conditions have influenced the evolution of the Denman and Scott ice streams.

In this work we study the geometry and tectonic setting of the KSSB to determine its origins and its subsequent modification by erosion. Using ICECAP data [*Blankenship et al.*, 2011, updated 2013, 2011, updated 2014, 2012, updated 2013a, 2012, updated 2013b, 2012, updated 2013c, 2014], we model the basin thickness and define the geometry of the most prominent basement structures. We compare our new results with the Perth and Mentelle Basins [*Borissova et al.*, 2010a; *Bradshaw et al.*, 2003; *Hall et al.*, 2013; *Mory and Iasky*, 1996; *Song and Cawood*, 2000] to contextualize basin formation within the breakup of East Gondwana. Finally, we estimate the amount of glacial erosion to assess how topographic and

tectonic conditions may have influenced the structure and evolution of the Denman and Scott glacier ice streams.

2. Geophysical Modeling

2.1. Tectonic Interpretation

We use a previous tectonic model of Wilkes Land [*Aitken et al*., 2014] as a starting point for our tectonic interpretation (Figure 1d), considering the following major basement elements: 1 - The Albany Fraser Province, bounded to the southeast by the Totten Fault and to the southwest by the Aurora Fault; 2 - The west Mawson Craton, bounded to the southwest by the Indo-Australo-Antarctic Suture (IAAS) [*Aitken et al*., 2014] and to the north by the Aurora and Totten Faults; 3 - The Bunger Hills Block, bounded to its east by the Scott Fault, is defined by a linear chain of high magnetic intensity anomalies (Figure 1b). These wrap around the northern end of the rift, encompassing the Obruchev and Bunger Hills outcrops (Figure 1d). 4 - The Indo-Antarctic Charcot Terrane lies east of the Bunger Hills Block and extends to the coast and potentially as far as Chugonov Island [*Sheraton*, 1995], and we demarcate this as the southernmost probable location of the IAAS (Figure 1d). The regions south of 70°S are poorly resolved, but generally are divided by the IAAS into Indo-Antarctic and Australo-Antarctic sectors.

The Knox Rift overprints these basement provinces, and is bounded to its west by the Scott Fault and to its east by the Conger Fault. The Knox Rift itself has some distinct gravity and magnetic characteristics. Broader, lower-amplitude anomalies beneath the KSSB define in general a relatively low-magnetization block, but a large rift-parallel positive anomaly also exists (Figure 1b). The basin has a strong negative free-air anomaly of -150 mGal, indicating thick sedimentary rocks, but also has smaller regions of higher gravity adjacent to the basin bounding Scott and Conger Faults, where the sedimentary basin is thinner (Figure 1a). To both sides of the rift, strong positive gravity anomalies mark the presence of exposed basement rocks at high elevation. Two flight lines cross an area of anomalously low gravity to the south, separated from the main gravity low by a gravity ridge (Figure 1a), and this is interpreted as an additional sub-basin.

Two dominant structural trends were identified from the geophysical dataset incorporating, firstly, the NNE trending basin-bounding Conger and Scott Faults and, secondly, the NW trending IAAS and Aurora Faults, as well as several smaller structures of each orientation. A third orientation (ENE) is observed within Australo-Antarctica, including the Totten Fault. Due to multiple reactivations, cross-cutting relationships between these structures are partly ambiguous; however, the ENE oriented structures (e.g. Totten) appear to be oldest, followed by the NW (e.g. IAAS and Aurora) and finally the NNE structures of the Knox Rift (e.g. Scott and Conger). Although the Scott and Conger Faults are not interrupted, variations in gravity and magnetic intensity along the rift axis suggest that the IAAS and associated structures have played an important role in rift evolution.

2.2. Gravity and Magnetic Modeling

To resolve further the crustal structure and basin thickness, 2D forward models were computed for seven flight-line profiles. Free-air gravity was used due to the explicit calculation of topographic effects, without assuming a particular density contrast. Air-ice and ice-rock surfaces correspond to the highest density contrast surfaces in the 2D models and, for the ICECAP dataset, regions of complex 3D topography generates non-systematic errors of ±500 m [*Aitken et al*., 2016a]. The filtering required to smooth aircraft accelerations, means that the free-air gravity data have a minimum resolvable half-wavelength of approximately 6-8 km, further exacerbating topographic effects in areas of steep topography. The total magnetic intensity data were sampled at high resolution, so wavelength sensitivity is dependent primarily on ice and sedimentary rock thicknesses. Both datasets were calculated at the aircraft flight elevation.

The initial model had five reference surfaces that existed across the entire model, namely the ice sheet surface, the ice-sheet bed, the KSSB base, an upper-crust/lower-crust boundary and the Moho. The Moho and a 13 km-thick lower crust were defined by a flexural model ($T_e = 25$ km) that accounts for the effect of depressed crust beneath ice and topographic loads.

The 2D forward modeling code calculates the integrated response from density/magnetization contrasts at manually delineated polygon boundaries [*Talwani et al*., 1959]. Polygon boundaries and internal properties were edited so as to fit the gravity and magnetic data but also minimizing the complexity of the model.

Table 1. Layered Structure of 2D Models With a Summary of Density and Susceptibility Values for Layers in the 2D Models

Layer	Density ρ (kg m^{-3})	Magnetic Susceptibility k (SI)	Reference
Air	0	0	
Ice	920	0	
Sedimentary Rocks (KSSB)	2400 (2200-2500)	0	*Delle Piane et al.* [2013]; *Iasky* [1993] – Perth Basin
Upper Crust	2600-2750	0.02-0.114	*Clark and Emerson* [1991]; *Goodwin* [1991]; *Hunt et al.* [1995]
Lower Crust	2800	0.01	*Tenzer and Bagherbandi* [2013]
Mantle	3200	0	*Tenzer and Bagherbandi* [2013]

For simplicity, and in the absence of local petrophysical knowledge, uniform magnetic susceptibility and density was assumed for the KSSB, lower crust and mantle (Table 1). The upper crust layer was subdivided into blocks corresponding to the main tectonic elements interpreted for the Knox Rift Region for which susceptibility and density were varied within reasonable limits (Table 1).

We assigned to the KSSB a sedimentary rock density of 2400 kg m^{-3}, but we tested a range of reasonable sedimentary rock densities between 2200 kg m^{-3} and 2500 kg m^{-3}. These values are similar to density values from the Perth Basin, including previous 2D gravity modeling studies [*Iasky*, 1993] and petrophysical measurements for Mesozoic sedimentary rocks [*Delle Piane et al*., 2013]. The other properties are permitted to change in line with global norms and regional data from Antarctica [*Tenzer and Bagherbandi*, 2013]. Full details of the 2D modeling work are provided in the supporting information.

The sensitivity of the modeled basin geometry to this density range is of the order of ±1-2 km, and scales linearly with the thickness of the basin. Final maps of the base of the sedimentary basin were generated at 10 km spatial resolution using, firstly, processing to remove declustering and secondly, interpolation by ordinary kriging with normal score transformation [*Oliver and Webster*, 1990]. The validity of the prediction map is confirmed by the acceptable prediction error [*Efron and Gong*, 1983] in the cross-validation statistics.

The models include density heterogeneities in the upper crust across the Knox Rift and IAAS. The Indo-Antarctic upper-crust is denser ($\rho = 2700$ kg m^{-3}), and apparently more uniform than the Australo-Antarctic upper-crust (ρ ranging between 2500 kg m^{-3} and 2700 kg m^{-3}). The tectonic heterogeneity of the Australo-Antarctic crust includes the difference between the Albany Fraser Province and the west Mawson Craton, as well as several intrusive suites. The Bunger Hills Block is a high-density block. Changes to the density and shape of the intra-basement boundaries add some degree of variability to the basin geometry but has little effect on the overall basin thickness.

2.3. Glacial Erosion Restoration Model

A 1D erosion restoration model was applied to study the isostatic modification of the basin geometry as result of both erosion and the growth of the EAIS. This restoration uses a method akin to sedimentary backstripping [*Watts and Ryan*, 1976] but applied in reverse. It provides, firstly, a better model of the initial basin morphology, but also helps to understand erosion processes in the Denman and Scott ice streams. Full details of the method are provided in the supporting information [*Jacobs and Lisker*, 1999; *Lisker et al*., 2007, 2014; *Mory and Iasky*, 1996; *Olierook et al*., 2016; *Taylor et al*., 2004].

In our approach we consider erosion in deep troughs, which reach over 1000 m below sea level, to be dominated by glacial erosion. Our model explicitly accounts for the glacial or subglacial fluvial erosion of sedimentary rocks and the isostatic effects of replacing those rocks with ice. This modeling was applied to the line-data along our model profiles, and the results were processed and interpolated in the same manner as the unadjusted basin-geometry results.

Sedimentary rocks are observed at elevations as high as 1000 m after glacial isostatic adjustment is applied, and we reconstruct a basin filled to that level.

Subaerial fluvial erosion from pre-glacial and inter-glacial periods is potentially a substantial component of the total erosion. We do not include it in this study due to the large uncertainty concerning past relative

sea level and therefore the potential limits on the depth and extent of subaerial erosion. Nevertheless, we can impose some bounds on the uncertainty.

Substantial subaerial erosion, if isostatically compensated, causes very large modifications to pre-erosion basin geometry, and from this we can infer that the degree of regionally extensive subaerial erosion is limited. Narrow and potentially deep river channels may have existed that would be either isostatically uncompensated, or supported by regional flexure [*Watts*, 2001]. Uncompensated valleys that are later filled with ice, eroded, and compensated are, isostatically speaking, identical to glacially eroded channels, and our approach models this scenario correctly.

Flexurally-supported valley incision (glacial or fluvial) will generate regional "up-warps" that cause our analysis to underestimate erosion outside of the trough, which is uplifted by more than in an isostatic model, and will overestimate erosion within the trough, which is uplifted by less than in an isostatic model. Flexural upwarps are typically low amplitude relative to the removed load [*Watts*, 2001].

3. Discussion and Conclusions

3.1. Basin Geometry

The basin structure consists of several depocenters arranged along the Knox Rift axis (Figure 1a). Adjusting basin geometry for ice loading and erosion-induced uplift, we further define the initial geometry of the basin (Figure 1c). The main depocenters are flanked to east and west by the Conger and Scott faults, but are also located between, and apparently controlled by, several NNW oriented fault segments relating to the IAAS.

The northernmost, depocenter A, is located adjacent to the Scott Fault, which forms a steep scarp. This depocenter currently reaches a maximum depth of 6.5 km (4 km thickness), and the basin may initially have been 6 – 7 km thick (Figure 1b - Model R24Ea). Depocenter B is further south, larger, and is located next to the Conger Fault. It currently reaches a depth of 6 km, similar to depocenter A (Figure 1b - Model R21Ea), although it may initially have been thicker (up to 8 km). Depocenter B has a lower basin-base gradient, and shallower-dipping margins compared to depocenter A. Two high-stand zones are identified on the margins of the main rift zone with low basin-base gradient and relatively shallow basement. High A is at the southwestern corner of the basin adjacent to the Scott Fault and contains up to 2 km of sedimentary rocks, having largely escaped erosion. High B is located at the north-eastern corner, with up to 3 km of sedimentary rocks adjacent to the Conger Fault, and is more heavily eroded (Figure 1b - Model R22Ea). The morphology of the basin base is consistent with two half-grabens with opposing polarity, bounded by the transtensional Scott and Conger faults, and segmented by the NNW-SSE trending structures.

Depocenter C lies south of the KSSB, and although the gravity data coverage does not allow to fully characterize this basin feature in 3D, our model suggests a total depth of over 4 km, with little overall erosion (Figure 1b - Model R19Wa).

Outside of these main depocenters, the northernmost part of the KSSB has smooth and relatively low bed topography suggesting sedimentary cover, but no deep accumulation of sedimentary rocks. Initial basin thickness may have been ~ 1-2 km. Similarly, a topographic ridge and gravity high between depocenters B and C may indicate a horst block, with initial basin thickness of up to 2 km.

3.2. Development of the Knox Subglacial Sedimentary Basin

The reconstructed basin geometry suggests the development of a transtensional pull-apart basin controlled by two prior structural trends (Figure 1a). The NNE oriented Conger and Scott Faults involve dextral oblique-normal kinematics, and the NNW-oriented structures are interpreted as scissor faults that segment the basin into discrete depocenters with opposing asymmetry. Furthermore, the topography and basin morphology of the rift indicates uplands to east and west, and lowlands to north and south, that can be separated by slip-lines [*Tapponnier and Molnar*, 1976] oriented NE-SW and NW-SE (Figure 1c). These kinematic criteria constrain the direction of maximum extension to N-S, with an error of not more than 10°. This well-constrained kinematic solution allows to interpret the Knox Rift evolution in the context of East Gondwana breakup reconstructions.

We use recently published reconstructions for the period between ~ 200 Ma and 130 Ma [*Gibbons et al*., 2012; *Seton et al*., 2012; *Williams et al*., 2011]. Although the full-fit Leeuwin/Hybrid model of *Williams et al*. [2011]

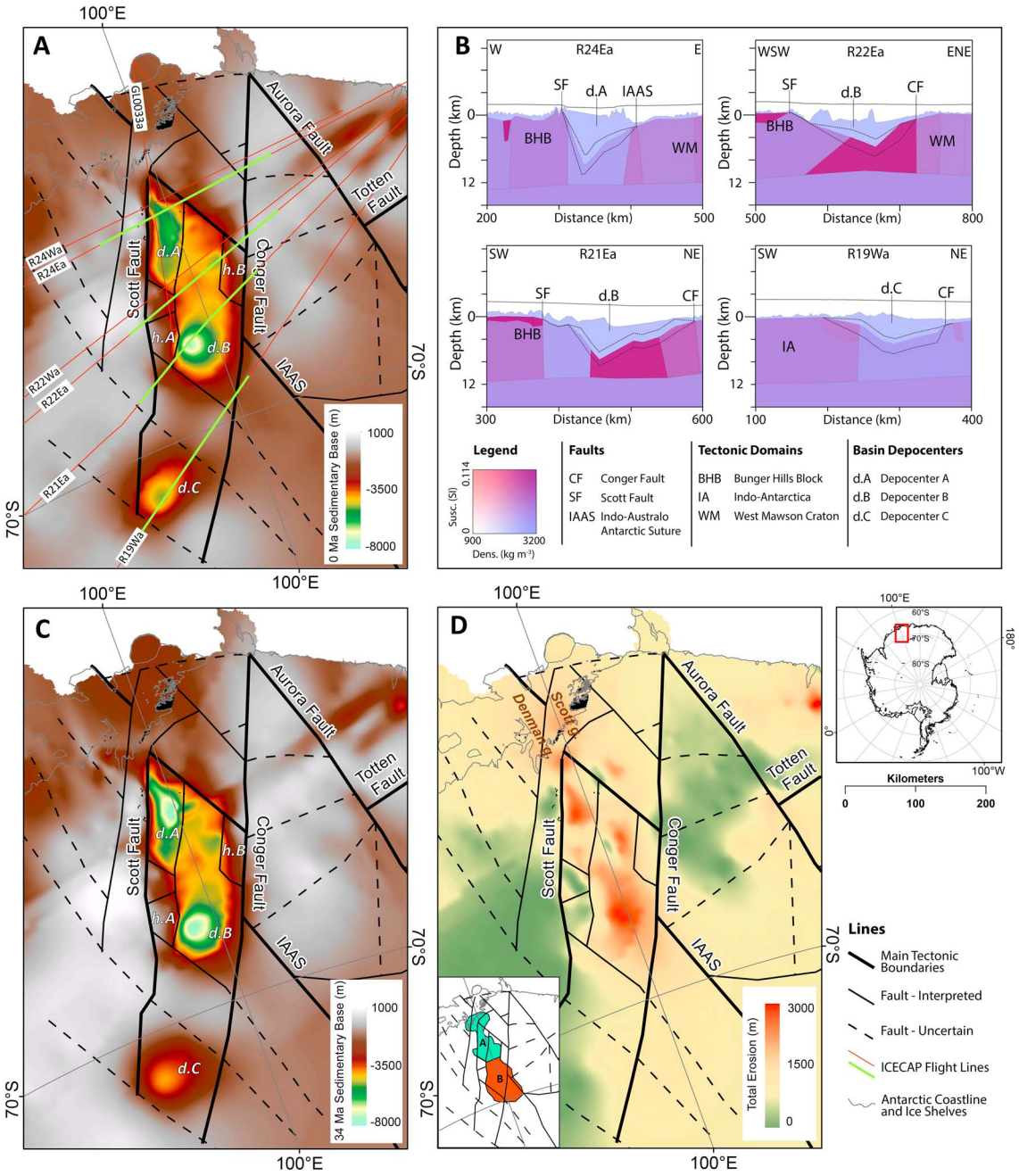

Figure 2. (a) WGS84 Elevation of the present-day KSSB base surface; (b) A detail of four representative 2D models along selected ICECAP flight lines (green); (c) Elevation of the KSSB base surface adjusted for erosion and glacial loading; (d) Total erosion estimate with the two interpreted erosion regions (inset on bottom-left).

(Figure 2a) aligns Precambrian structures well [*Aitken et al.*, 2014], including the Darling-Conger Fault, it is perhaps not representative of the fit at 200 Ma as it results in unacceptable continental overlap between Tasmania and Antarctica [*Whittaker et al.*, 2013].

These reconstructions place the Knox Rift along strike from initially the Perth Basin, and later the Mentelle Basin (Figure 2). These basins record two main phases of rifting and subsidence: rift phase I occurred in the late Permian-Triassic and rift phase II occurred in the late Jurassic-Cretaceous.

Rift phase I is interpreted to have resulted from a large-scale plate reorganization, driven by Cimmerian rifting events at the Tethyan margin of Pangea [*Ali et al.*, 2013] and by the Gondwanide

Orogeny at the Pacific margin [*Cawood*, 2005; *Cawood and Buchan*, 2007]. Permo-Triassic depocenters are present along the west Australian margin, notably in the Perth and Southern Carnarvon Basins, as well as on the Greater India margin [*Mukhopadhyay et al*., 2010]. In the Perth Basin, this rift phase resulted in E-W extension, followed by structural inversion, uplift and erosion [*Song and Cawood*, 2000], also extending to the small Collie Basin [*Lowry*, 1976] and to the eastern sector of the Mentelle Basin [*Borissova et al*., 2010a]. The kinematics of rift phase I do not explain the main subsidence pattern in the KSSB, and we suggest that the KSSB was isolated from this rifting. We suggest that a significant dextral motion on the Aurora Fault [*Aitken et al*., 2016b] accommodated this differential extension and the offset of the Conger Fault relative to the Darling Fault. This motion aligns the KSSB with the Mentelle Basin prior to Late Jurassic to Early Cretaceous rifting (Figure 2b).

Rift phase II results from the Late Jurassic–Early Cretaceous rifting of Greater India from East Gondwana and is widely recognizable in sedimentary basins along the East Gondwana rifting margins. In the Perth Basin, this second rift phase caused segmentation of the basin along NW trending transfer zones following the main extensional vector for East Gondwana breakup. Rift Phase II also involved dextral strike-slip movement along the Darling Fault [*Song and Cawood*, 2000] with kinematics consistent with those interpreted for the KSSB. Extension in the Mentelle Basin resumed in the Mid-Jurassic, generating a series of extensional half graben depocenters in the western Mentelle Basin and persisting until sea-floor spreading developed at 132 Ma [*Borissova et al*., 2010b]. Our interpreted kinematics for the main subsidence phase of the KSSB are consistent with not only the direction of Indian plate motion post-breakup, but also the kinematics of rift phase II within the Perth and western Mentelle Basins [*Borissova et al*., 2010b; *Song and Cawood*, 2000]. The formation of the KSSB is thus constrained to the Late Jurassic–Early Cretaceous (Figure 2c), and was along-strike from and likely coeval with the western Mentelle Basin.

The spatial link with the developing plate-margin, may have been abandoned after 132 Ma, when sea-floor spreading developed in the region of the Mentelle Basin [*Borissova et al*., 2010b], and the locus of rifting shifted to the south-west [*Gaina et al*., 2007; *Gibbons et al*., 2013]. The Indo-Antarctic margin preserves rift-basins associated with this rifting phase, continuing until seafloor spreading commenced at 129 Ma [*Gaina et al*., 2007; *Seton et al*., 2012] (Figure 2d). Extension in the Knox Rift may have continued through this period in an intraplate setting, with no direct link to the plate margin. Although poorly dated, the post-rift Shackleton Basin was formed over new oceanic crust after 129 Ma [*Stagg et al*., 2005], and the Knox Rift may also preserve a similarly-aged post-rift subsidence phase.

3.3. Erosion of the Knox Subglacial Sedimentary Basin

By taking into account current ice thickness, glacial erosion and the isostatic equilibration of those, the erosion restoration model provides the first opportunity to assess the role of the interpreted basin structures in the dynamics and evolution of the Denman and Scott Glaciers. We interpret two main erosion regions in the Knox Rift (Figure 1d). Region A is located in the coastal part of the KSSB, and connects to the Denman and Scott glaciers. Region A contains elevated highlands with rough surfaces and deeply incised fjords with smoother beds (Figure 1c). Elsewhere within Antarctica, this pattern of rough highs and smooth, narrow lows (fjords) has been interpreted to result from highlands being protected from glacial erosion due to cold-based ice, whereas valleys focus both fluvial and glacial erosion [*Rippin et al*., 2014; *Ross et al*., 2014; *Jamieson et al*., 2014; *Young et al*., 2011]. Highly selective erosion is suggested, perhaps driven by a high degree of flow-convergence into these fjords from a thick mass of ice upstream, in region B. Region B is located deeper inland, above depocenter B, and is also deeply eroded, but without fjords. This erosion may represent activity of the Denman and Scott streams during less extensive phases in the evolution of the ice sheet (Figure 3).

Mapped erosion is focused within the rift (Figure 1d), and the distribution within the rift zone shows a strong correlation with the major depocenters, where it is highest. The link with the main depocenters suggests that topographic focusing [*Winsborrow et al*., 2010] and a mechanically-weak and probably wet sedimentary bed [*Wright et al*., 2012; *Gooch et al*., 2016] may have focused the ice-stream within the rift zone, as has been suggested for ice streams in West Antarctica [*Bingham et al*., 2012]. The past history of the Denman and Scott ice streams is not known well, but our results suggest that fast-flowing, warm-based ice has rarely impacted the regions outside of the rift axis, and this constraint is likely to remain in the future.

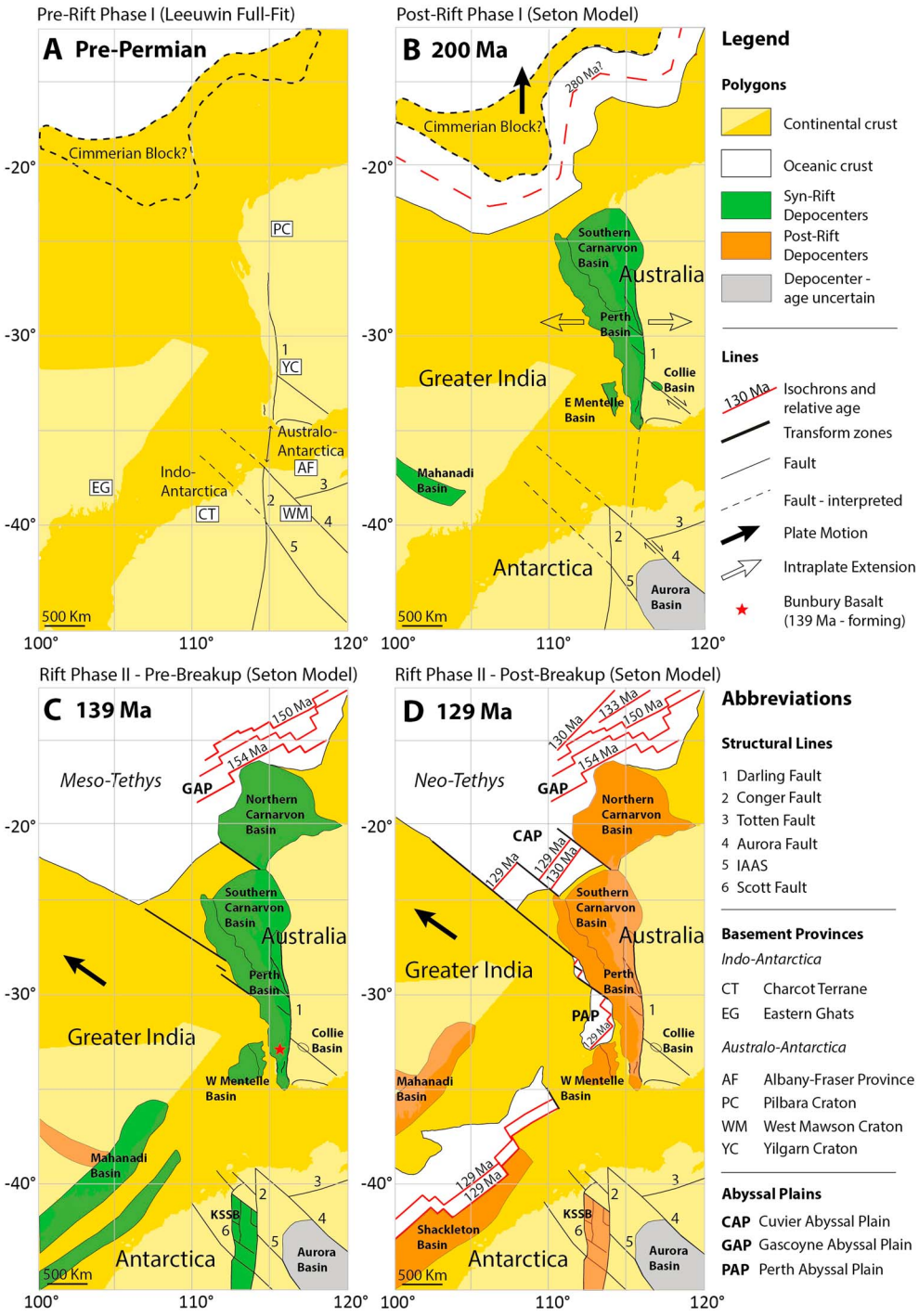

Figure 3. Mercator-projected reconstructions of East Gondwana. (a) Pre-Permian full-fit Leeuwin/Hybrid reconstruction as in *Aitken et al.* [2014] showing the alignment of the Precambrian Darling and Conger Faults; (b) Post-rift phase I reconstruction (200 Ma). Relative eastwards motion of Australo-Antarctica in rift phase I forms the Perth Basin and offsets the Darling and Conger faults, re-aligning the Knox Rift with the Mentelle Basin. Dextral motion along the Aurora Fault accommodates the differential motion with Antarctica; (c) Pre-breakup (rift phase II – 139 Ma) reconstruction showing the formation of the KSSB, driven by extension along the vector of Indian plate motion; (d) Post-breakup (129 Ma) reconstruction with potentially ongoing extension and subsidence in the Knox Rift. Models were constructed in GPlates [*Williams et al.*, 2012] with Australia fixed in present-day coordinates.

Acknowledgments

This work forms the result of AM's MSc thesis, for which support was provided by the School of Earth and Environment of the University of Western Australia. ARAA was supported for this work by the UWA Goodeve Foundation. Collection of ICECAP data was supported by: National Science Foundation grant PLR-0733025; National Aeronautics and Space Administration grants NNX09AR52G, NNG10HPO6C and NNX11AD33G (Operation Ice Bridge and the American Recovery and Reinvestment Act); Australian Antarctic Division projects 3013 and 4077; National Environment and Research Council grant NE/D003733/1; the Jackson School of Geosciences; the G. Unger Vetlesen Foundation; and the Australian Government's Cooperative Research Centres Programme through the Antarctic Climate & Ecosystems Cooperative Research Centre (ACE CRC). ICECAP data products used in this study are available in the supporting information and through the ICEBRIDGE data portal at the National Snow and Ice Data Center (http://nsidc.org/icebridge/portal/). We thank Annette George, Mike Dentith and the two reviewers for their constructive comments and helpful suggestions on an earlier version of the manuscript.

References

Aitken, A. R. A., D. A. Young, F. Ferraccioli, P. G. Betts, J. S. Greenbaum, T. G. Richter, J. L. Roberts, D. D. Blankenship, and M. J. Siegert (2014), The subglacial geology of Wilkes Land, East Antarctica, *Geophys. Res. Lett.*, *41*, 2390–2400, doi:10.1002/2014GL059405.

Aitken, A. R. A., J. L. Roberts, T. D. van Ommen, D. A. Young, N. R. Golledge, J. S. Greenbaum, D. D. Blankenship, and M. J. Siegert (2016a), Repeated large-scale retreat and advance of Totten Glacier indicated by inland bed erosion, *Nature*, *533*(7603), 385–389, doi:10.1038/nature17447.

Aitken, A. R. A., P. G. Betts, D. A. Young, D. D. Blankenship, J. L. Roberts, and M. J. Siegert (2016b), The Australo-Antarctic Columbia to Gondwana transition, *Gondwana Res.*, *29*(1), 136–152, doi:10.1016/j.gr.2014.10.019.

Ali, J. R., H. M. C. Cheung, J. C. Aitchison, and Y. Sun (2013), Palaeomagnetic re-investigation of Early Permian rift basalts from the Baoshan Block, SW China: Constraints on the site-of-origin of the Gondwana-derived eastern Cimmerian terranes, *Geophys. J. Int.*, *193*(2), 650–663, doi:10.1093/gji/ggt012.

Bingham, R. G., F. Ferraccioli, E. C. King, R. D. Larter, H. D. Pritchard, A. M. Smith, and D. G. Vaughan (2012), Inland thinning of West Antarctic Ice Sheet steered along subglacial rifts, *Nature*, *487*(7408), 468–471, doi:10.1038/nature11292.

Blankenship, D. D., S. D. Kempf, and D. A. Young (2011, updated 2013), IceBridge HiCARS 1 L2 Geolocated Ice Thickness, version 1, NASA Distributed Active Archive Center (DAAC) at the National Snow and Ice Data Center (NSIDC), doi:10.5067/F5FGUT9F5089.

Blankenship, D. D., D. A. Young, T. G. Richter, and J. S. Greenbaum (2011, updated 2014), IceBridge BGM-3 Gravimeter L2 Geolocated Free Air Anomalies, version 1, NASA Distributed Active Archive Center (DAAC) at the National Snow and Ice Data Center (NSIDC), doi:10.5067/8DJW56PKY133.

Blankenship, D. D., et al. (2012, updated 2013a), IceBridge Riegl Laser Altimeter L2 Geolocated Surface Elevation Triplets, version 1, NASA Distributed Active Archive Center (DAAC) at the National Snow and Ice Data Center (NSIDC), doi:10.5067/JV9DENETK13E.

Blankenship, D. D., S. D. Kempf, and D. A. Young (2012, updated 2013b), IceBridge HiCARS 2 L2 Geolocated Ice Thickness, version 1, NASA Distributed Active Archive Center (DAAC) at the National Snow and Ice Data Center (NSIDC), doi:10.5067/9EBR2T0VXUDG.

Blankenship, D. D., S. D. Kempf, and D. A. Young (2012, updated 2013c), IceBridge Geometrics 823A Cesium Magnetometer L1B Time-Tagged Magnetic Field, version 1, NASA Distributed Active Archive Center (DAAC) at the National Snow and Ice Data Center (NSIDC), doi:10.5067/9WRB1GVWBU7O.

Blankenship, D. D., D. A. Young, T. G. Richter, and J. S. Greenbaum (2014), IceBridge CMG GT-1A Gravimeter L2 Geolocated Free Air Gravity Disturbances, version 1, NASA Distributed Active Archive Center (DAAC) at the National Snow and Ice Data Center (NSIDC), doi:10.5067/3X4CIKKSYQRU.

Borissova, I., B. E. Bradshaw, C. J. Nicholson, D. S. Payne, and H. I. M. Struckmeyer (2010a), Mentelle Basin - Tectonic Evolution Controlled by of the Combined Extensional History of the Southwestern and Southern Australian Margins paper presented at 21st ASEG-PESA Conference and exhibition, Sydney, 22-26 August 2010.

Borissova, I., B. E. Bradshaw, C. J. Nicholson, D. S. Payne, and H. I. M. Struckmeyer (2010b), New exploration opportunities on the southwest Australian margin – deep-water frontier Mentelle Basin, *Aust. Pet. Prod. Explor. Assoc. J.*, *50*, 1–13.

Bradshaw, B. E., N. Rollet, J. M. Totterdell, and I. Borissova (2003), A revised structural framework for frontier basins on the southern and southwestern Australian continental margin Geoscience Australia, Record 2003/03, pp. 3-27.

Cawood, P. A. (2005), Terra Australis Orogen: Rodinia breakup and development of the Pacific and Iapetus margins of Gondwana during the Neoproterozoic and Paleozoic, *Earth Sci. Rev.*, *69*(3), 249–279, doi:10.1016/j.earscirev.2004.09.001.

Cawood, P. A., and C. Buchan (2007), Linking accretionary orogenesis with supercontinent assembly, *Earth Sci. Rev.*, *82*(3), 217–256, doi:10.1016/j.earscirev.2007.03.003.

Chand, S., M. Radhakrishna, and C. Subrahmanyam (2001), India–East Antarctica conjugate margins: Rift-shear tectonic setting inferred from gravity and bathymetry data, *Earth Planet. Sci. Lett.*, *185*(1), 225–236, doi:10.1016/S0012-821X(00)00349-6.

Clark, D., and D. Emerson (1991), Notes on rock magnetization characteristics in applied geophysical studies, *Explor. Geophys.*, *22*(3), 547–555, doi:10.1071/EG991547.

Close, D. I., H. M. J. Stagg, and P. E. O'Brien (2007), Seismic stratigraphy and sediment distribution on the Wilkes Land and Terre Adélie margins, East Antarctica, *Mar. Geol.*, *239*(1), 33–57, doi:10.1016/j.margeo.2006.12.010.

Delle Piane, C., L. Esteban, N. Timms, and S. Ramesh Israni (2013), Physical properties of Mesozoic sedimentary rocks from the Perth Basin, Western Australia, *Aust. J. Earth Sci.*, *60*(6-7), 735–745, doi:10.1080/08120099.2013.831948.

Efron, B., and G. Gong (1983), A Leisurely Look at the Bootstrap, the Jackknife, and Cross-Validation, *Am. Stat.*, *37*(1), 36–48, doi:10.2307/2685844.

Espurt, N., J. Callot, F. Roure, J. M. Totterdell, H. I. M. Struckmeyer, and R. Vially (2012), Transition from symmetry to asymmetry during continental rifting: An example from the Bight Basin–Terre Adélie Australian and Antarctic conjugate margins, *Terra Nova*, *24*(3), 167–180, doi:10.1111/j.1365-3121.2011.01055.x.

Fitzsimons, I. C. W. (2003), Proterozoic basement provinces of southwestern Australia, and their correlation with Antarctica, in *Proterozoic East Gondwana: Supercontinent Assembly and Breakup*, edited by Y. Yoshida, B. F. Windley, and S. Dasgupta, *Geol. Soc. Spec. Publ.*, 206, 93–130, doi:10.1144/GSL.SP.2003.206.01.07.

Frederick, B. C., D. A. Young, D. D. Blankenship, T. G. Richter, S. D. Kempf, F. Ferraccioli, and M. J. Siegert (2016), Distribution of subglacial sediments across the Wilkes Subglacial Basin, East Antarctica, *J. Geophys. Res. Earth Surf.*, *121*, 790–813, doi:10.1002/2015JF003760.

Gaina, C., R. Müller, B. Brown, T. Ishihara, and S. Ivanov (2007), Breakup and early seafloor spreading between India and Antarctica, *Geophys. J. Int.*, *170*(1), 151–169, doi:10.1111/j.1365-246X.2007.03450.x.

Gibbons, A. D., U. Barckhausen, P. Van Den Bogaard, K. Hoernle, R. Werner, J. M. Whittaker, and R. D. Müller (2012), Constraining the Jurassic extent of Greater India: Tectonic evolution of the West Australian margin, *Geochem. Geophys. Geosyst.*, *13*, Q05W13, doi:10.1029/2011GC003919.

Gibbons, A. D., J. M. Whittaker, and R. D. Muller (2013), The breakup of East Gondwana: Assimilating constraints from Cretaceous ocean basins around India into a best-fit tectonic model, *J. Geophys. Res. Solid Earth*, *118*, 808–822, doi:10.1002/jgrb.50079.

Gooch, B. T., D. A. Young, and D. D. Blankenship (2016), Potential groundwater and heterogeneous heat source contributions to ice sheet dynamics in critical submarine basins of East Antarctica, *Geochem. Geophys. Geosyst.*, *17*, 395–409, doi:10.1002/2015GC006117.

Goodwin, A. M. (1991), *Precambrian Geology, the Dynamic Evolution of the Continental Crust*, pp. 359–450 , Academic Press, London.

Hall, L. S., A. D. Gibbons, G. Bernadel, J. M. Whittaker, C. Nicholson, N. Rollet, and R. D. Müller (2013), Structural Architecture of Australia's Southwest Continental Margin and Implications for Early Cretaceous Basin Evolution, West Australian Basins Symposium 2013 proceedings Petroleum Exploration Society of Australia Limited, pp. 1-22.

Hunt, C. P., B. M. Moskowitz, and S. K. Banerjee (1995), Magnetic properties of Rocks and Minerals, in *Rock Physics and Phase Relations: A Handbook of Physical Constants*, edited by T. J. Ahrens, AGU, Washington, D. C., doi:10.1029/RF003p0189.

Iasky, R. P. (1993), A structural study of the southern Perth Basin Geol. Surv. of Western Australia, Rep. 31, p. 56.
Jacobs, J., and F. Lisker (1999), Post Permian tectono-thermal evolution of western Dronning Maud Land, East Antarctica: An apatite fission-track approach, *Antarct. Sci.*, *11*(4), 451–460, doi:10.1017/S0954102099000589.
Jamieson, S. S. R., C. R. Stokes, N. Ross, D. M. Rippin, R. G. Bingham, D. S. Wilson, M. Margold, and M. J. Bentley (2014), The glacial geomorphology of the Antarctic ice sheet bed, *Antarct. Sci.*, *26*(6), 724–741, doi:10.1017/s0954102014000212.
Lisker, F., H. Gibson, C. J. Wilson, and A. Läufer (2007), Denudation and uplift of the Mawson Escarpment (eastern Lambert Graben, Antarctica) as indicated by apatite fission track data and geomorphological observation U.S. Geol. Surv. Open File Rep., 2007-1047-SRP-105.
Lisker, F., J. Prenzel, A. L. Läufer, and C. Spiegel (2014), Recent thermochronological research in northern Victoria Land, Antarctica, *Polarforschung*, *84*(1), 59–66.
Lowry, D. C. (1976), Tectonic history of the Collie Basin, Western Australia, *J. Geol. Soc. Aust.*, *23*(1), 95–104, doi:10.1080/00167617608728923.
Mory, A. J., and R. P. Iasky (1996), Stratigraphy and structure of the onshore northern Perth Basin Geol. Surv. of Western Australia, Rep. 46, p. 101.
Mukhopadhyay, G., S. K. Mukhopadhyay, M. Roychowdhury, and P. Parui (2010), Stratigraphic correlation between different Gondwana Basins of India, *J. Geol. Soc. India*, *76*(3), 251–266, doi:10.1007/s12594-010-0097-6.
Olierook, H. K., F. E. Jourdan, R. R. Merle, N. Timms, J. Muhling, and N. Kusznir (2016), Bunbury Basalt: Gondwana breakup products or earliest vestiges of the Kerguelen mantle plume?, *Earth Planet. Sci. Lett.*, *440*, 20–32, doi:10.1016/j.epsl.2016.02.008.
Oliver, M. A., and R. Webster (1990), Kriging: A method of interpolation for geographical information systems, *Int. J. Geogr. Inf. Syst.*, *4*(3), 313–332, doi:10.1080/02693799008941549.
Rignot, E., J. Mouginot, and B. Scheuchl (2011), Ice Flow of the Antarctic Ice Sheet, *Science*, *333*(6048), 1427–1430, doi:10.1126/science.1208336.
Rippin, D. M., R. G. Bingham, T. A. Jordan, A. P. Wright, N. Ross, H. F. J. Corr, F. Ferraccioli, A. M. Le Brocq, K. C. Rose, and M. J. Siegert (2014), Basal roughness of the Institute and Möller Ice Streams, West Antarctica: Process determination and landscape interpretation, *Geomorphology*, *214*, 139–147, doi:10.1016/j.geomorph.2014.01.021.
Ross, N., T. A. Jordan, R. G. Bingham, H. F. J. Corr, F. Ferraccioli, A. Le Brocq, D. M. Rippin, A. P. Wright, and M. J. Siegert (2014), The Ellsworth Subglacial Highlands: Inception and retreat of the West Antarctic Ice Sheet, *Geol. Soc. Am. Bull.*, *126*(1-2), 3–15, doi:10.1130/b30794.1.
Seton, M., et al. (2012), Global continental and ocean basin reconstructions since 200 Ma, *Earth Sci. Rev.*, *113*(3–4), 212–270, doi:10.1016/j.earscirev.2012.03.002.
Sheraton, J. W. (1995), Geology of the Bunger Hills-Denman Glacier region, East Antarctica Australian Geological Survey Organisation, Bulletin 244, p. 124.
Song, T., and P. A. Cawood (2000), Structural styles in the Perth Basin associated with the Mesozoic break-up of Greater India and Australia, *Tectonophysics*, *317*(1), 55–72, doi:10.1016/S0040-1951(99)00273-5.
Stagg, H. M. J., J. B. Colwell, N. G. Direen, P. E. O'Brien, B. J. Browning, G. Bernardel, I. Borissova, L. Carson, and D. I. Close (2005), Geological framework of the continental margin in the region of the Australian Antarctic Territory Geoscience Australia, Record, 2004/2, pp. 1-373.
Talwani, M., L. Worzel, and M. Landisman (1959), Rapid gravity computations for two-dimensional bodies with application to the Mendocino Submarine Fracture Zone, *J. Geophys. Res.*, *64*(1), 49–59, doi:10.1029/JZ064i001p00049.
Tapponnier, P., and P. Molnar (1976), Slip-line field theory and large-scale continental tectonics, *Nature*, *264*(5584), 319–324, doi:10.1038/264319a0.
Taylor, J., M. J. Siegert, A. J. Payne, M. J. Hambrey, P. E. O'Brien, A. K. Cooper, and G. Leitchenkov (2004), Topographic controls on post-Oligocene changes in ice-sheet dynamics, Prydz Bay region, East Antarctica, *Geology*, *32*(3), 197–200, doi:10.1130/G20275.1.
Tenzer, R., and M. Bagherbandi (2013), Reference crust-mantle density contrast beneath Antarctica based on the Vening Meinesz-Moritz isostatic inverse problem and CRUST2.0 seismic model, *Earth Sci. Res. J.*, *17*(1), 7–12, doi:10.1007/s11200-011-0023-7.
Watts, A. B. (2001), *Isostasy and Flexure of the Lithosphere*, Cambridge Univ. Press, Cambridge, U. K.
Watts, A. B., and W. B. F. Ryan (1976), Flexure of the lithosphere and continental margin basins, *Tectonophysics*, *36*(1), 25–44, doi:10.1016/0040-1951(76)90004-4.
Whittaker, J. M., S. E. Williams, and R. D. Müller (2013), Revised tectonic evolution of the Eastern Indian Ocean, *Geochem. Geophys. Geosyst.*, *14*, 1891–1909, doi:10.1002/ggge.20120.
Williams, S. E., J. M. Whittaker, and R. D. Müller (2011), Full-fit, palinspastic reconstruction of the conjugate Australian-Antarctic margins, *Tectonics*, *30*, TC6012, doi:10.1029/2011TC002912.
Williams, S. E., R. D. Müller, T. C. W. Landgrebe, and J. M. Whittaker (2012), An open-source software environment for visualizing and refining plate tectonic reconstructions using high-resolution geological and geophysical data sets, *Geol. Soc. Am.*, *22*(4), 4–9.
Winsborrow, M. C. M., C. D. Clark, and C. R. Stokes (2010), What controls the location of ice streams?, *Earth Sci. Rev.*, *103*(1), 45–59, doi:10.1016/j.earscirev.2010.07.003.
Wright, A. P., et al. (2012), Evidence of a hydrological connection between the ice divide and ice sheet margin in the Aurora Subglacial Basin, East Antarctica, *J. Geophys. Res.*, *117*, F01033, doi:10.1029/2011JF002066.
Young, D. A., et al. (2011), A dynamic early East Antarctic Ice Sheet suggested by ice-covered fjord landscapes, *Nature*, *474*(7349), 72–75, doi:10.1038/nature10114.